SUPPLEMENTARY MATERIAL: Effective elastic moduli of space-filled multi-material composite lattices

T. Mukhopadhyay[1,*], S. Naskar[1], D. Kundu[2], S. Adhikari[3]

[1] *Faculty of Engineering and Physical Sciences, University of Southampton, Southampton SO17 1BJ, UK*
[2] *Department of Aerospace Engineering, Indian Institute of Technology Kanpur, Kanpur, India*
[3] *James Watt School of Engineering, University of Glasgow, Glasgow G12 8QQ, UK*
[*] *Email address: T.Mukhopadhyay@soton.ac.uk*

Abstract

In this document we provide the detailed derivation of beam stiffness matrix based on two different approaches (conventional element stiffness matrix and exact element stiffness matrix), followed by the derivation of effective elastic moduli of the lattices in terms of the beam-level element stiffness matrix. We also present supplementary numerical results for the two Young's moduli, shear modulus and Poisson's ratios considering auxetic and non-auxetic configurations.

Contents

S1. Element stiffness matrices

Stiffness matrix of an equivalent beam element is derived here following two different approaches: conventional element stiffness matrix approach and exact element stiffness matrix approach.

S1.1. Conventional element stiffness matrix

The governing equation of transverse deflection $V(x)$ of a beam can be expressed as

$$EI\frac{d^4V(x)}{dx^4} + kV(x) = f(x) \tag{S1}$$

We assume here that the beams under consideration follow the Euler-Bernoulli hypotheses and the elastic infill is modelled as an equivalent elastic contribution of the filler material throughout the beam length [1]. In the above equation, EI denotes the bending rigidity and k is the equivalent elastic filler modulus, while length of the beam is L. Here we assume that the reaction force arising from the filler material is proportional to the transverse deformation of the constituent beams. However, other relationships between the reaction force and the transverse deformation could also be considered following the current framework.

An element of the beam is shown in figure 1(D) of the main paper, which has four degrees of freedom and there are four shape functions. The degrees-of-freedom for each node include a vertical and a rotational component. The conventional shape function matrix considering bending deformation [2] can be represented in terms of cubic polynomials as shown below. The continuous shape functions give an idea about how different displacement functions will vary in between the discrete values at the nodes over the elements.

$$\mathbf{N}(x) = [N_1(x), N_2(x), N_3(x), N_4(x)]^T \tag{S2}$$

where

$$\begin{aligned} N_1(x) &= 1 - 3\frac{x^2}{L^2} + 2\frac{x^3}{L^3}, \qquad & N_2(x) &= x - 2\frac{x^2}{L} + \frac{x^3}{L^2}, \\ N_3(x) &= 3\frac{x^2}{L^2} - 2\frac{x^3}{L^3}, & N_4(x) &= -\frac{x^2}{L} + \frac{x^3}{L^2} \end{aligned} \tag{S3}$$

Subsequently, the stiffness matrix of a beam with equivalent elastic contribution of the filler material can be obtained using the usual variational formulation [3] as

$$\begin{aligned} \mathbf{K}_e &= EI\int_0^L \frac{d^2\mathbf{N}(x)}{dx^2}\frac{d^2\mathbf{N}^T(x)}{dx^2}\mathrm{d}x + k\int_0^L \mathbf{N}(x)\mathbf{N}^T(x)\mathrm{d}x \\ &= \frac{EI}{L^3}\begin{bmatrix} 12 & 6L & -12 & 6L \\ 6L & 4L^2 & -6L & 2L^2 \\ -12 & -6L & 12 & -6L^2 \\ 6L & 2L^2 & -6L & 4L^2 \end{bmatrix} + \frac{kL}{420}\begin{bmatrix} 156 & 22L & 54 & -13L \\ 22L & 4L^2 & 13L & -3L^2 \\ 54 & 13L & 156 & -22L \\ -13L & -3L^2 & -22L & 4L^2 \end{bmatrix} \end{aligned} \tag{S4}$$

For the special case when the there is no elastic filler material (i.e. $k = 0$), the stiffness matrix derived above approaches to the classical stiffness matrix of a beam [2, 3].

S1.2. Exact element stiffness matrix

The cubic polynomials, used as the shape functions above, are not the exact solutions of the governing differential equation (S1). They are exact only when $k = 0$. The main idea in this section is to employ shape functions which satisfy the governing differential equation exactly. To obtain the characteristic equation, we consider the response of the form

$$V(x) = \exp[\lambda x] \tag{S5}$$

Substituting this in the governing equation (S1) one obtains

$$EI\lambda^4 + k = 0 \quad \text{or} \quad \lambda^4 = -\frac{k}{EI} \tag{S6}$$

Solving the above equation, four solutions for λ can be expressed as

$$\lambda_{1,2,3,4} = \left(\frac{1}{\sqrt{2}} + \mathrm{i}\frac{1}{\sqrt{2}}\right)\sqrt[4]{\frac{k}{EI}}, \left(\frac{1}{\sqrt{2}} - \mathrm{i}\frac{1}{\sqrt{2}}\right)\sqrt[4]{\frac{k}{EI}}, \tag{S7}$$

$$-\left(\frac{1}{\sqrt{2}} + \mathrm{i}\frac{1}{\sqrt{2}}\right)\sqrt[4]{\frac{k}{EI}}, -\left(\frac{1}{\sqrt{2}} - \mathrm{i}\frac{1}{\sqrt{2}}\right)\sqrt[4]{\frac{k}{EI}}, \tag{S8}$$

These can be concisely expressed as

$$\lambda_{1,2,3,4} = (\pm 1 \pm \mathrm{i})\, b \tag{S9}$$

where

$$b = \sqrt[4]{\frac{k}{4EI}} \tag{S10}$$

Next we use these solutions to obtain the shape functions of the beam.

Transcendental shape functions

The transcendental shape functions are obtained in a way that the equation of dynamic equilibrium is exactly satisfied at all points within the beam element. Similar to the classical finite element method, we assume that the transverse displacement within an element is interpolated from the nodal displacements as

$$V_e(x) = \mathbf{N}^T(x)\widehat{\mathbf{V}}_e \tag{S11}$$

Here $\widehat{\mathbf{V}}_e$ is the nodal displacement vector $\mathbf{N}(x)$ is the vector of shape functions and $n = 4$ is the number of the nodal degrees-of-freedom. Suppose the $s_j(x), j = 1, \cdots, 4$ are the basis functions which exactly satisfy equation (S1). We express the shape function vector as a linear combination of basis vectors so that

$$\mathbf{N}(x) = \mathbf{\Gamma}\mathbf{s}(x) \tag{S12}$$

where the matrix $\mathbf{\Gamma}$ depends on the boundary conditions. The elements of $\mathbf{s}(x)$ are constituted of $\exp[\lambda_j x]$ where the values of λ_j are obtained from the solution of the characteristics equation as given in equation (S9).

Based on the solutions in equation (S9), the displacement field within the beam element can be expressed using a linear combination of the basic functions involved in $e^{\lambda_j x}$. Ignoring the signs, we have

$$e^{(1+\mathrm{i})bx} = e^{bx}e^{\mathrm{i}bx} = \{\cosh(bx) + \sinh(bx)\}\{\cos(bx) + \mathrm{i}\sin(bx)\} \tag{S13}$$

$$= \underbrace{\mathrm{i}\sin(bx)\sinh(bx)}_{s_1(x)} + \underbrace{\mathrm{i}\sin(bx)\cosh(bx)}_{s_2(x)} + \underbrace{\cos(bx)\sinh(bx)}_{s_3(x)} + \underbrace{\cos(bx)\cosh(bx)}_{s_4(x)} \tag{S14}$$

The transcendental functions $s_j(x), j = 1, \cdots, 4$ defined above are the exact basis functions which can be used to represent any displacement field within the element. The vector $\mathbf{s}(x)$ therefore, is expressed as

$$\mathbf{s}(x) = \begin{Bmatrix} \sin(bx)\sinh(bx) \\ \sin(bx)\cosh(bx) \\ \cos(bx)\sinh(bx) \\ \cos(bx)\cosh(bx) \end{Bmatrix} \tag{S15}$$

The displacement field within the element can be expressed as

$$V_e(x) = \mathbf{s}(x)^T\mathbf{V}_e \tag{S16}$$

where $\mathbf{V}_e$ is the vector of constants, which can be determined from boundary conditions.

The relationship between the shape functions and the boundary conditions can be represented as in Table S1, where boundary conditions in each column give rise to the corresponding shape function. Writing equation (S16) for the above four sets of boundary conditions, one obtains Writing equation (S16) for the above four sets of boundary conditions, one obtains

Table S1: The relationship between the boundary conditions and the shape functions for transverse bending deflection of beams.

	$N_1(x,\omega)$	$N_2(x,\omega)$	$N_3(x,\omega)$	$N_4(x,\omega)$
$V(0)$	1	0	0	0
$\frac{dV(x)}{dx}(0)$	0	1	0	0
$V(L)$	0	0	1	0
$\frac{dV(x)}{dx}(L)$	0	0	0	1

$$[\mathbf{R}]\left[\mathbf{V}_e^1, \mathbf{V}_e^2, \mathbf{V}_e^3, \mathbf{V}_e^4\right] = \mathbf{I} \tag{S17}$$

where $\mathbf{V}_e^k$ is the vector of constants that gives rise to the kth shape function and $\mathbf{I}$ is a 4×4 identity matrix. The matrix $\mathbf{R}$ can be obtained as

$$\begin{aligned}\mathbf{R} &= \begin{bmatrix} s_1(0) & s_2(0) & s_3(0) & s_4(0) \\ \frac{ds_1(x)}{dx}(0) & \frac{ds_2(x)}{dx}(0) & \frac{ds_3(x)}{dx}(0) & \frac{ds_4(x)}{dx}(0) \\ s_1(L) & s_2(L) & s_3(L) & s_4(L) \\ \frac{ds_1(x)}{dx}(L) & \frac{ds_2(x)}{dx}(L) & \frac{ds_3(x)}{dx}(L) & \frac{ds_4(x)}{dx}(L) \end{bmatrix} \\ &= \begin{bmatrix} 0 & 0 & 0 & 1 \\ 0 & b & b & 0 \\ sS & sC & cS & cC \\ cbS + sCb & cbC + sSb & -sSb + cbC & -sCb + cbS \end{bmatrix}\end{aligned} \tag{S18}$$

Here following notations are used to simplify the expressions

$$C = \cosh(bL), \quad c = \cos(bL), \quad S = \sinh(bL) \quad \text{and} \quad s = \sin(bL) \tag{S19}$$

Based on the boundary conditions represented in Table S1 and equation (S17), the shape functions can be expressed by equation (S12) where

$$\mathbf{\Gamma} = \left[\mathbf{V}_e^1, \mathbf{V}_e^2, \mathbf{V}_e^3, \mathbf{V}_e^4\right]^T = \left[\mathbf{R}^{-1}\right]^T \tag{S20}$$

By obtaining the matrix $\mathbf{\Gamma}$ from the above equation, the shape function vector can be obtained from equation (S12). After some algebraic simplifications, we can represent the transcendental shape functions as

$$\begin{Bmatrix} N_1(x,\omega) \\ N_2(x,\omega) \\ N_3(x,\omega) \\ N_4(x,\omega) \end{Bmatrix} = \frac{1}{Ab} \begin{bmatrix} -b\,(C^2 - c^2) & b\,(SC + sc) & -b\,(SC + sc) & bA \\ -SC + sc & C^2 - 1 & -1 + c^2 & 0 \\ 2\,sSb & -b\,(cS + sC) & b\,(cS + sC) & 0 \\ -sC + cS & sS & -sS & 0 \end{bmatrix} \begin{Bmatrix} \sin(bx)\sinh(bx) \\ \sin(bx)\cosh(bx) \\ \cos(bx)\sinh(bx) \\ \cos(bx)\cosh(bx) \end{Bmatrix} \tag{S21}$$

Here the constant A is given by

$$A = \sinh^2(bL) - \sin^2(bL) = S^2 - s^2 \tag{S22}$$

and b is defined in equation (S10).

Transcendental element stiffness matrix

The stiffness matrix can be developed following the conventional variational formulation [3]. The main difference is instead of the classical cubic polynomials as the shape functions, transcendental shape functions in (S21) should be used. It is convenient to have the overall stiffness matrix as

$$\mathbf{D}_e = EI\mathbf{K}_{1e} + k\mathbf{K}_{2e} \tag{S23}$$

where

$$\mathbf{K}_{1e} = \int_0^L \frac{d^2\mathbf{N}(x,\omega)}{dx^2}\frac{d^2\mathbf{N}^T(x,\omega)}{dx^2}\mathrm{d}x \tag{S24}$$

$$\text{and} \quad \mathbf{K}_{2e} = \int_0^L \mathbf{N}(x,\omega)\mathbf{N}^T(x,\omega)\mathrm{d}x \tag{S25}$$

Using the expression of b from (S10), we have $k = 4b^4EI$. Substituting this in equation (S23) we have the transcendental stiffness matrix

$$\mathbf{K}_e = EI\left(\mathbf{K}_{1e} + 4b^4\mathbf{K}_{2e}\right) \tag{S26}$$

Using the expressions of the shape functions from the previous subsection, after few algebraic simplifications the stiffness matrix of an individual beam element with equivalent elastic contribution of the filler material can be given by the following closed-form expression

$$\mathbf{D}_e = \frac{2EIb}{(S^2-s^2)}\begin{bmatrix} 2\,b^2\,(SC+sc) & b\,(C^2-c^2) & -2\,b^2\,(cS+sC) & 2\,sSb \\ b\,(C^2-c^2) & SC-sc & -2\,sSb & sC-cS \\ -2\,b^2\,(cS+sC) & -2\,sSb & 2\,b^2\,(SC+sc) & -b\,(C^2-c^2) \\ 2\,sSb & sC-cS & -b\,(C^2-c^2) & SC-sc \end{bmatrix} \tag{S27}$$

The elements of this matrix are transcendental functions of (bL).

S2. Effective elastic moduli of in-filled lattices in terms of beam stiffness matrix

The effective elastic moduli of hexagonal honeycomb-like cellular materials without any infill was obtained in published literature [4] as

$$E_{1_{\mathrm{GA}}} = E\left(\frac{t}{l}\right)^3 \frac{\cos\theta}{(\frac{h}{l}+\sin\theta)\sin^2\theta} \tag{S28}$$

$$E_{2_{\mathrm{GA}}} = E\left(\frac{t}{l}\right)^3 \frac{(\frac{h}{l}+\sin\theta)}{\cos^3\theta} \tag{S29}$$

$$\nu_{12_{\mathrm{GA}}} = \frac{\cos^2\theta}{(\frac{h}{l}+\sin\theta)\sin\theta} \tag{S30}$$

$$\nu_{21_{\mathrm{GA}}} = \frac{(\frac{h}{l}+\sin\theta)\sin\theta}{\cos^2\theta} \tag{S31}$$

$$\text{and} \quad G_{12_{\mathrm{GA}}} = E\left(\frac{t}{l}\right)^3 \frac{(h/l+\sin\theta)}{\left(\frac{h}{l}\right)^2(1+2\frac{h}{l})\cos\theta} \tag{S32}$$

Our aim in this section is to obtain similar closed-form expressions when the lattices is filled with an elastic material. In the preceding section, we have derived the element stiffness matrices for a single beam with the equivalent effect of space-filling based on two different methods (exact element stiffness and conventional stiffness). From these stiffness matrices, analytical expressions of the in-plane elastic moduli are obtained in this section. For the purpose of deriving such expressions for the space-filled lattices, the element stiffness matrix is re-written in the following general form

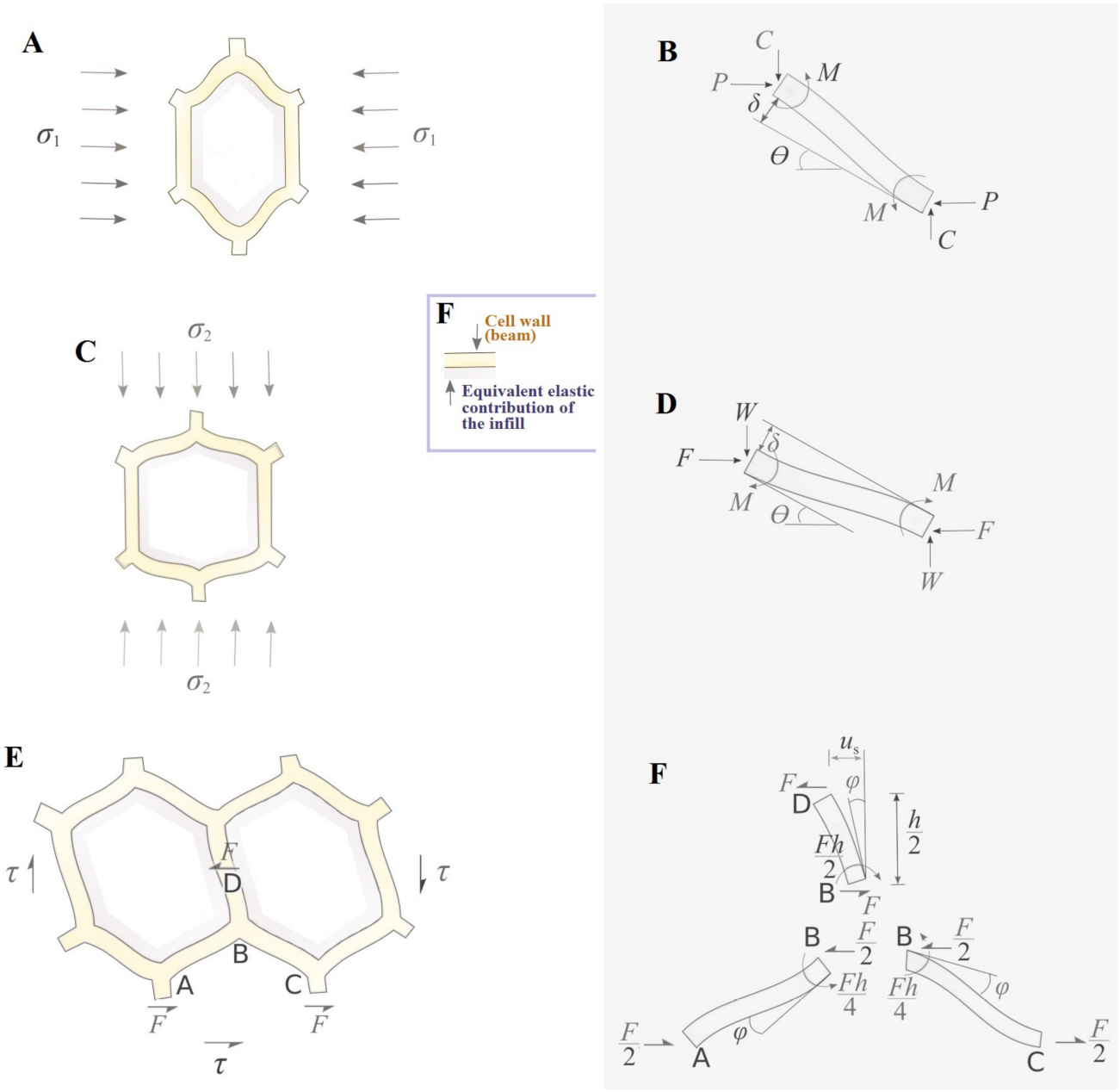

Fig. S1: Mechanics of filled honeycombs. For analysing the space-filled honeycombs we consider the idealized unit cells as shown in figure 1(CII). Note that the connecting members of an idealized unit cell consists of a beam (cell wall) and an equivalent elastic contribution of the infill material. **(A)** Deformed shape of idealized honeycombs under the application of stress in direction - 1. In the present analysis, we consider direction-1 in the direction perpendicular to the axis of the vertical member. Direction- 2 is perpendicular to direction - 1. Material of the cell walls and the equivalent elastic contribution of the infill are indicated using two different colours in figures 2(A, C, E). However, for better understanding of the mechanics, we only schematically show the outlines of the deformed beams in figures 2(B, D, E). It should be kept in mind that the configuration of these schematic beam elements are same as shown in figure 2(F). **(B)** Free body diagram of a slant member, the deformation of which predominantly contributes to the in-plane Young's moduli of the lattice structure. **(C)** Deformed shape of idealized honeycombs under the application of stress in direction - 2. **(D)** Free body diagram of a slant member that predominantly contributes to Young's modulus in direction - 2. **(E)** Deformed shape of idealized honeycombs under the application of in-plane shear stress. **(F)** Free body diagram of the vertical and slant members that contribute to the in-plane shear modulus. Note here that the deformation mechanics of the idealized beam members in the free-body diagrams (B, D and F) are governed by the compound effect of the stiffness contributions of the cell wall as well as the equivalent elastic contribution of the infill.

$$\mathbf{D}_e = [A_{ij}]_{4\times4} \tag{S33}$$

where $i, j = 1, 2, 3, 4$. The terms of the above matrix have the expressions corresponding to the terms of equation (S27) (for exact element stiffness matrix) and equation (S4) (for conventional stiffness matrix).

S2.1. Derivation of Young's modulus E_1

One cell wall is considered for deriving the expression of Young's modulus E_1 under the application of stress in direction - 1 as shown in figure S1(A-B) [4]. In the free body diagram of the slant member in figure S1(B), the rotational displacements of both ends and the bending displacement of one end is considered as zero. To satisfy the equilibrium of forces in direction 2, the force C is needed to be zero. Thus from the general stiffness matrix presented in equation (S33), the bending deflection of one end of the slant member with respect to the other end can be written as

$$\delta = \frac{P \sin\theta}{A_{33}} \tag{S34}$$

where $P = \sigma_1(h + l\sin\theta)\bar{b}$ (geometric dimensions of a single honeycomb cell is shown in figure 1(B-C) of the main paper. $\bar{b}$ is the width of the beam i.e. thickness of the honeycomb sheet). The component of δ in direction 1 is $\delta \sin\theta$. Thus the strain component in direction - 1 due to applied stress in the same direction can be expressed as

$$\begin{aligned} \epsilon_{11} &= \frac{\delta \sin\theta}{l\cos\theta} \\ &= \frac{\sigma_1(h + l\sin\theta)\bar{b}\sin^2\theta}{A_{33} l\cos\theta} \end{aligned} \tag{S35}$$

Using this, the Young's modulus E_1 can be explicitly expresses in terms of the A_{33} element of the stiffness matrix as

$$E_1 = \frac{\sigma_1}{\epsilon_{11}} = \frac{A_{33} l\cos\theta}{(h + l\sin\theta)\bar{b}\sin^2\theta} \tag{S36}$$

S2.2. Derivation of Young's modulus E_2

Similar to the derivation of E_1, the bending deformation of one end of the slant beam under the application of σ_2 (as shown in figure S1(C-D)) can be expressed as

$$\delta = \frac{W\cos\theta}{A_{33}} \tag{S37}$$

where $W = \sigma_2 l\bar{b}\cos\theta$. The expression for strain component in direction 2 due to application of stress in the same direction can be obtained as

$$\begin{aligned} \epsilon_{22} &= \frac{\delta\cos\theta}{(h + l\sin\theta)} \\ &= \frac{\sigma_2 l\bar{b}\cos^3\theta}{A_{33}(h + l\sin\theta)} \end{aligned} \tag{S38}$$

Using this, like the previous subsection, the Young's modulus E_2 can also be explicitly expresses in terms of the A_{33} element of the stiffness matrix as

$$E_2 = \frac{\sigma_2}{\epsilon_{22}} = \frac{A_{33}(h + l\sin\theta)}{l\bar{b}\cos^3\theta} = \frac{A_{33}}{\bar{b}} \frac{(\frac{h}{l} + \sin\theta)}{\cos^3\theta} \tag{S39}$$

S2.3. Derivation of Poisson's ratios ν_{12} and ν_{21}

Poisson's ratio is defined as the negative ratio of strains normal to, and parallel to, the loading direction. Poisson's ratio ν_{12} can be obtained under loading in direction 1 as

$$\epsilon_{12} = -\frac{\epsilon_{21}}{\epsilon_{11}} \tag{S40}$$

where ϵ_{11} and ϵ_{21} represent the strains in direction 1 and direction 2 respectively, under the loading in direction 1. The strain ϵ_{11} can be obtained from the first part of Equation (S35), while ϵ_{21} can be written as

$$\epsilon_{21} = \frac{-\delta\cos\theta}{(h + l\sin\theta)} \tag{S41}$$

Expression for Poisson's ratio due to loading in direction 1 can be expressed as

$$\nu_{12} = \frac{\cos^2\theta}{(\eta + \sin\theta)\sin\theta} \tag{S42}$$

Similarly the expression for Poisson's ratio due to loading in direction - 2 can be expressed as

$$\nu_{21} = \frac{(\eta + \sin\theta)\sin\theta}{\cos^2\theta} \tag{S43}$$

S2.4. Derivation of shear modulus G_{12}

For deriving the expression of G_{12}, two members of the honeycomb cell are needed to be considered (vertical member with length $\frac{h}{2}$ and a slant member with length l) as shown in figure S1(E-F). The points A, B and C will not have any relative movement due to the symmetrical structure. The total shear deflection u_s consists of two components, bending deflection of the member BD and its deflection due to rotation of joint B.

It can be noted here that the elements of the general stiffness matrix (refer to equation(S33)) will be different for the vertical member and the slant member due to their different lengths. Using the stiffness components of the general stiffness matrix, the bending deformation of point D with respect to point B in direction 1 can be obtained as

$$\delta_b = \frac{F}{\left(A^v_{33} - \frac{A^v_{34}A^v_{43}}{A^v_{44}}\right)} \tag{S44}$$

where $F = 2\tau l\bar{b}\cos\theta$. The superscript v in the elements of the stiffness matrix is used to indicate the stiffness element corresponding to the vertical member.

From the free body diagram presented in figure S1(F),

$$M = \frac{Fh}{4} \tag{S45}$$

On the basis of equation (S33), deflection of the end B with respect to the end C due to application of moment M at the end B is given as

$$\delta_r = \frac{M}{A^s_{43}} \tag{S46}$$

where the superscript s in A_{43} is used to indicate the stiffness element corresponding to the slant member. Thus the rotation of joint B can be expressed as

$$\begin{aligned} \phi &= \frac{\delta_r}{l} \\ &= \frac{Fh}{4lA^s_{43}} \end{aligned} \tag{S47}$$

Total shear deformation under the application of shear stress τ can be expressed as

$$\begin{aligned} u_s &= \frac{1}{2}\phi h + \delta_b \\ &= \frac{Fh^2}{8lA^s_{43}} + \frac{F}{\left(A^v_{33} - \dfrac{A^v_{34}A^v_{43}}{A^v_{44}}\right)} \end{aligned} \tag{S48}$$

The shear strain is given by

$$\begin{aligned} \gamma &= \frac{2u_s}{(h + l\sin\theta)} \\ &= \frac{F}{(h + l\sin\theta)}\left(\frac{h^2}{4lA^s_{43}} + \frac{2}{\left(A^v_{33} - \dfrac{A^v_{34}A^v_{43}}{A^v_{44}}\right)}\right) \\ &= \frac{2\tau l\bar{b}\cos\theta}{(h + l\sin\theta)}\left(\frac{h^2}{4lA^s_{43}} + \frac{2}{\left(A^v_{33} - \dfrac{A^v_{34}A^v_{43}}{A^v_{44}}\right)}\right) \end{aligned} \tag{S49}$$

Due to the symmetry of the element stiffness matrix $A^v_{34} = A^v_{43}$. Using this, we can further simplify to obtain

$$G_{12} = \frac{\tau}{\gamma} = \frac{(\frac{h}{l} + \sin\theta)}{\bar{b}\cos\theta}\frac{1}{\left(\frac{h^2}{2lA^s_{43}} + \dfrac{4A^v_{44}}{A^v_{44}A^v_{33} - (A^v_{34})^2}\right)} \tag{S50}$$

Equations S36, S39 and S50 are the closed-form expressions of two Young's moduli and shear modulus in terms of elements of the general stiffness matrix of a beam. We will utilise these expressions to obtain the elastic moduli in terms of the geometric and intrinsic material parameters for the case of conventional stiffness matrix and the transcendental stiffness matrix. Equations S42 and S43 represent the Poisson's ratios, where we notice that these quantities are not dependent on the elements of the beam stiffness matrix.

S3. Supplementary numerical results

In this section we present additional numerical results for the five elastic moduli to investigate the effects of geometric and intrinsic material parameters considering auxetic and non-auxetic configurations. Figure S2 shows variation of Young's moduli with α along with infill stiffness and γ. Note that the non-dimensional ratio of Young's modulus presented here are not dependent on η and cell angle θ. Thus the numerical results are applicable for any values of η and different auxetic and non-auxetic configurations. Figure S3 shows variation of in-plane shear modulus with α and η along with infill stiffness and γ. Note that the non-dimensional ratio of shear modulus presented here are not dependent on cell angle θ. Thus the numerical results are applicable for different auxetic and non-auxetic configurations. The contour plots reveal that while the trends of variation remains similar, the values of elastic moduli varies significantly with geometric and intrinsic material parameters. Further, the elastic moduli can be modulated and enhanced significantly as a function of the infill stiffness even with low-density filler materials.

As noted in the preceding section, the in-plane Poisson's ratios are not dependent on the components of the beam stiffness matrix, and thus the infill material. Variations of Poisson's ratios are shown in figure S4 considering auxetic and non-auxetic configurations. The feasibility of manufacturing the auxetic structures is taken into account while presenting the results as (refer to figure 1(C) of the main paper)

$$h/l \geq 2\sin\theta \tag{S51}$$

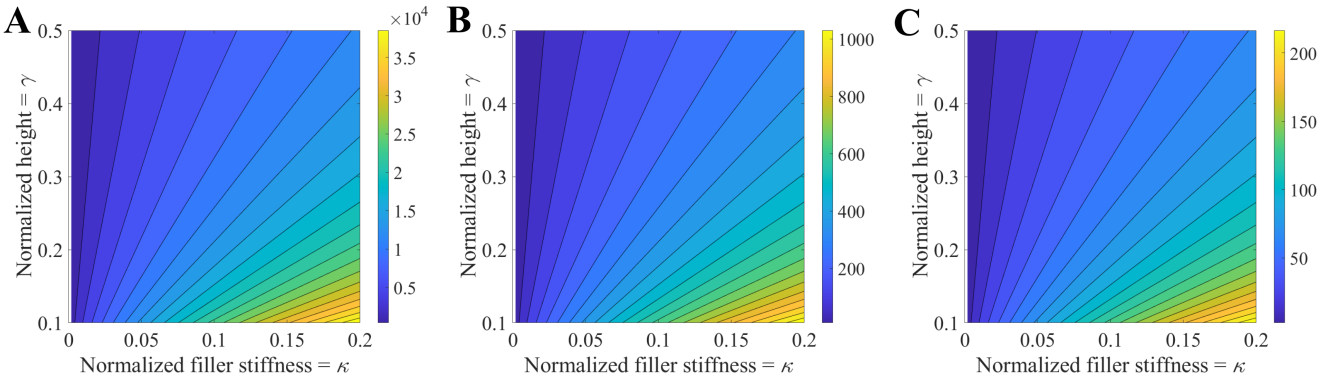

Fig. S2: The interaction effect of filler stiffness and height ratios on the Young's moduli. Normalised Young's moduli $E_i/E_{i_{\mathrm{GA}}}$ (where $i = 1, 2$) are plotted as a function of the filler stiffness ratio $\kappa = k/E$ and the height ratio $\gamma = \bar{b}/l$. Three values of the thickness ratio $\alpha = 0.01$, 0.05 and 0.1 are considered. Note that although the expressions of E_1 and E_2 are different, the ratios $E_1/E_{1_{\mathrm{GA}}}$ and $E_2/E_{2_{\mathrm{GA}}}$ are the same. Thus we present only one plot that represents the results of both the Young's moduli. The actual value of the two Young's moduli, which are different, can be obtained by multiplying the presented numerical values by the corresponding Young's modulus of unfilled lattices. The subscript GA is used to indicate the elastic moduli obtained based on the case of unfilled honeycomb lattices [4]. Note that $E_i/E_{i_{\mathrm{GA}}}$ is not dependent on η, meaning these results are applicable to any value of η. **(A)** Thickness ratio $\alpha = 0.01$ **(B)** Thickness ratio $\alpha = 0.05$ **(C)** Thickness ratio $\alpha = 0.1$.

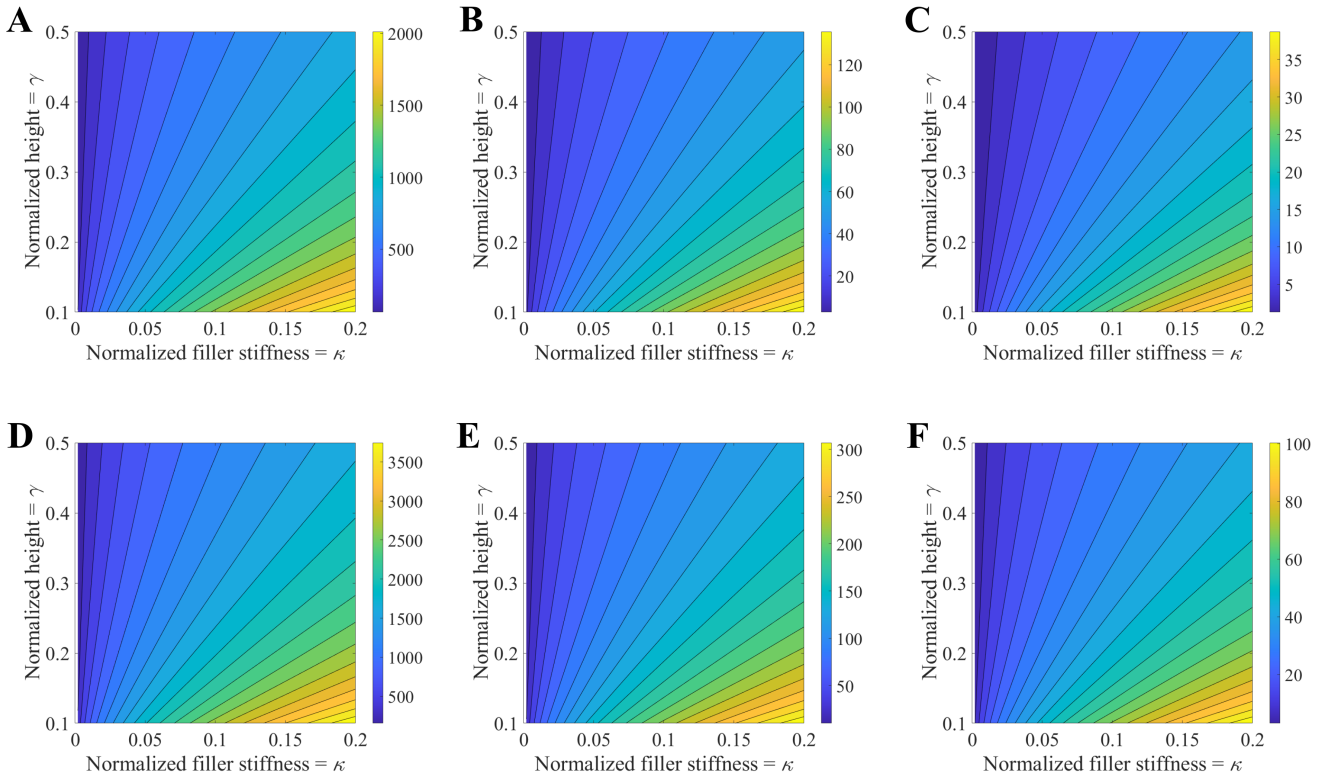

Fig. S3: The interaction effect of filler stiffness and height ratios on the in-plane shear modulus. Normalised shear modulus $G_{12}/G_{12_{\mathrm{GA}}}$ is plotted as a function of the filler stiffness ratio $\kappa = k/E$ and the height ratio $\gamma = \bar{b}/l$. Three values of the thickness ratio $\alpha = 0.01$, 0.05 and 0.1, and two values of $\eta = h/l = 1, 2$ are considered. The subscript GA is used to indicate the elastic moduli obtained based on the case of unfilled honeycomb lattices [4]. **(A, D)** Microstructural configuration: $\alpha = 0.01$ with $\eta = 1$ and $\eta = 2$. **(B, E)** Microstructural configuration: $\alpha = 0.05$ with $\eta = 1$ and $\eta = 2$. **(C, F)** Microstructural configuration: $\alpha = 0.1$ with $\eta = 1$ and $\eta = 2$.

Note that the same inequality is also applicable to the results presented in figures S2 and S3 for the Young's moduli and shear modulus.

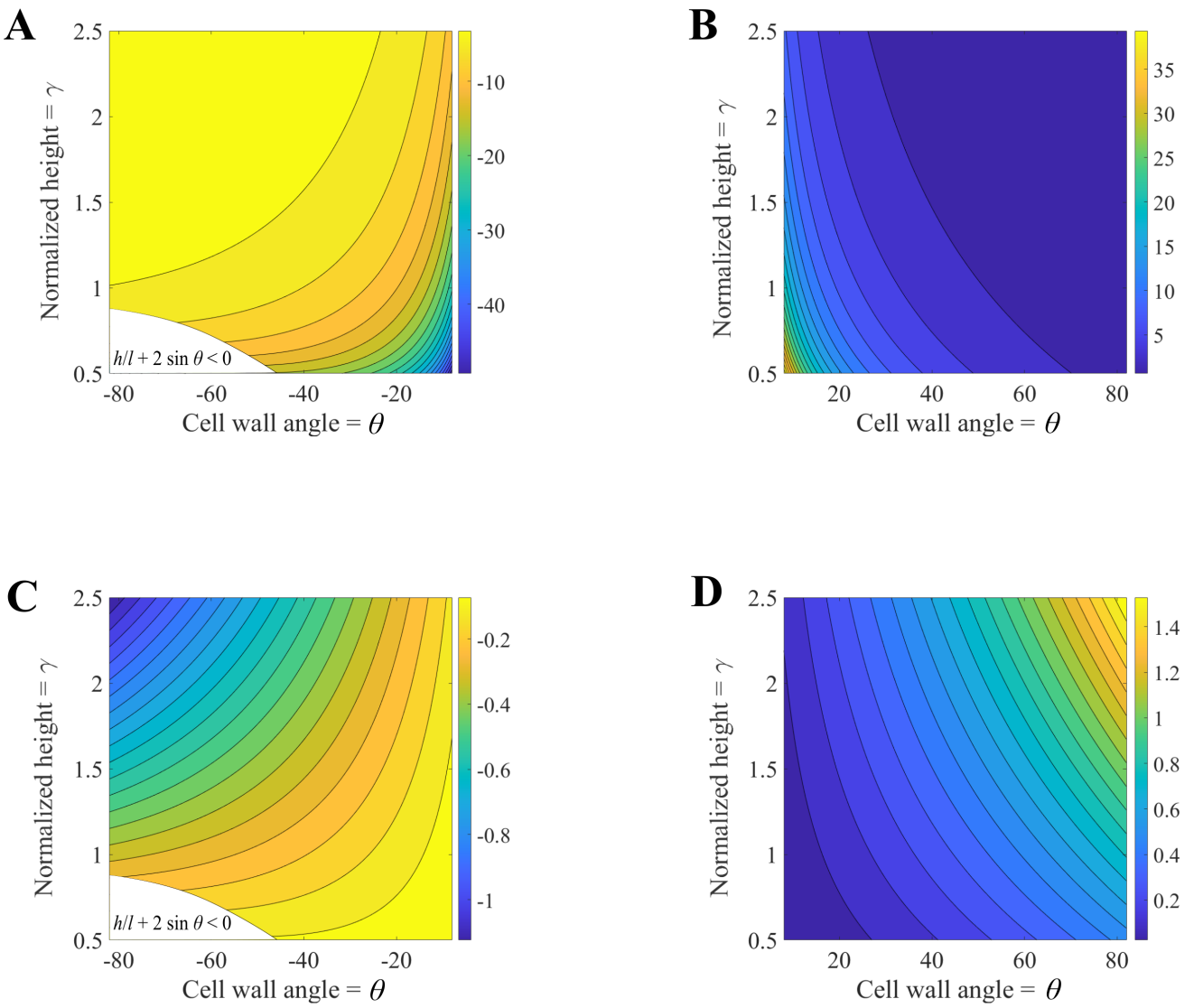

Fig. S4: The interaction effect of cell wall angle and height ratios on the in-plane Poisson's ratios. The Poisson's ratios are not dependent upon the normalized filler stiffness ratio $\kappa = k/E$. **(A, C)** Poisson's ratios, ν_{12} and ν_{21} for auxetic lattices. **(B, D)** Poisson's ratios, ν_{12} and ν_{21} for non-auxetic lattices.

Acknowledgments

TM and SN acknowledge the initiation grant received from University of Southampton.

References

[1] Manohar C, Adhikari S. 1998 Dynamic stiffness of randomly parametered beams. *Probabilistic Engineering Mechanics* **13**, 39 – 51.

[2] Petyt M. 1998 *Introduction to Finite Element Vibration Analysis*. Cambridge, UK: Cambridge University Press.

[3] Dawe D. 1984 *Matrix and Finite Element Displacement Analysis of Structures*. Oxford, UK: Oxford University Press.

[4] Gibson, L., Ashby, M. F., 1999. Cellular Solids Structure and Properties. Cambridge University Press, Cambridge, UK.